Accepted Manuscript

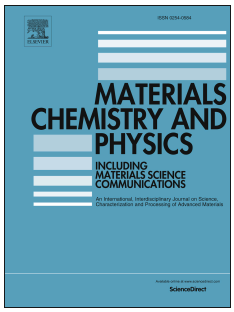

Selective and sensitive detection of L-Cysteine via fluorometric assay using gold nanoparticles and Rhodamine B in aqueous medium

Pradip Maiti, Tanmoy Singha, Utsav Chakraborty, Sannak Dutta Roy, Parimal Karmakar, Bapi Dey, Syed Arshad Hussain, Sharmistha Paul, Pabitra Kumar Paul

PII: S0254-0584(19)30500-0

DOI: https://doi.org/10.1016/j.matchemphys.2019.06.001

Reference: MAC 21708

To appear in: *Materials Chemistry and Physics*

Received Date: 26 February 2019

Revised Date: 30 May 2019

Accepted Date: 3 June 2019

Please cite this article as: P. Maiti, T. Singha, U. Chakraborty, S.D. Roy, P. Karmakar, B. Dey, S.A. Hussain, S. Paul, P.K. Paul, Selective and sensitive detection of L-Cysteine via fluorometric assay using gold nanoparticles and Rhodamine B in aqueous medium, *Materials Chemistry and Physics* (2019), doi: https://doi.org/10.1016/j.matchemphys.2019.06.001.

TOC graphic

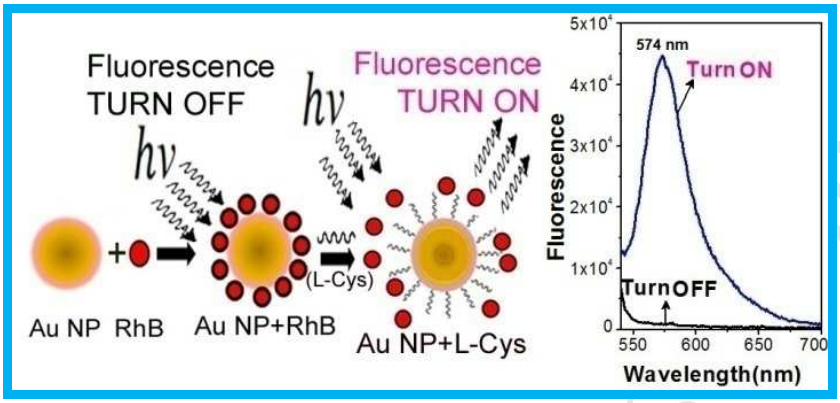

Detection of L- Cysteine by using fluorometric assay

Selective and Sensitive Detection of L-Cysteine via Fluorometric assay using Gold Nanoparticles and Rhodamine B in Aqueous Medium

Pradip Maiti[a,b], Tanmoy Singha[a], Utsav Chakraborty[a], Sannak Dutta Roy[a], Parimal Karmakar[c], Bapi Dey[d], Syed Arshad Hussain[d], Sharmistha Paul[b*] and Pabitra Kumar Paul[a*]

a. Department of Physics, Jadavpur University, Jadavpur, Kolkata-700032, India

b. West Bengal State Council of Science and Technology, Department of Higher education, Science and Technology and Biotechnology, Vigyan Chetana Bhavan, Sector-I, Salt Lake, Kolkata-700064, India

c. Department of Life Science & Bio-technology, Jadavpur University, Jadavpur, Kolkata-700032, India

d. Department of Physics, Tripura University, Suryamaninagar-799022, Tripura West, India

……..

* Corresponding author

*Email: pkpaul@phys.jdvu.ac.in (P.K. Paul), sharmistha.paul@gov.in (S. Paul)

Phone: +91-9477631142 (M), +91-33-24138917 (O)

FAX: +91-33-24138917 (O)

Abstract

An assay method based on fluorometric and colorimetric change was developed for selective sensing of important thiol containing amino acid L-Cysteine (L-Cys) by using gold nanoparticles (Au NPs) and Rhodamine B (RhB) in aqueous environment. This fluorometric assay is basically relies on the competitive binding between RhB and Au NPs via electrostatic interaction as well as strong thiol(-SH)-Au NPs bonding via chemisorption. Citrate stabilized Au NPs (diameter ~27 nm) was synthesized by soft chemical method and characterized by UV-Vis absorption spectroscopy and Transmission electron microscopic (TEM) techniques. The change in non-radiative energy transfer between RhB and Au NPs are responsible for the observed drastic fluorescence quenching of RhB via FRET process. The recovery of fluorescence from the assay solution of RhB/Au NPs after addition of L-Cys was found linear over the concentration range 0.01 µM to 1000 µM with experimental limit of detection (LOD) of 0.01 µM. The selective interaction of L-Cys with the mixed solution of RhB/Au NPs was reflected by the color change from wine to bluish-black of the final solution. The proposed fluorometric assay method accompanied with the observed colorimetric change could successfully differentiate other interfering amino acids including thiol (-SH) containing compounds namely L-Methionine, L-Homocysteine and antioxidant glutathione with the high degree of accuracy. Also the LOD is comparable to the concentration of L-Cys present in the blood plasma. The proposed sensing mechanism is also confirmed with pure human urine sample to detect the response of L-Cys in the urine. Therefore, this fluorometric assay technique for detection of L-Cys has great potential with the diagnostic impact for biomedical interest.

Keywords: Gold nanoparticle, Rhodamine B, Amino acids, Colorimetric/fluorometric, L-Cysteine, Urine

1. Introduction

The thiol containing amino acid L-Cys generally found in human plasma is well known as the building block of proteins and is involved in verity of important biological processes [1]. Normally a small amount of L-Cys is present in human body in the form of N-acetyl-L-cysteine (NAC) commonly known as L-Cys and is naturally derived from the amino acids serine and methionine [2]. It is widely used in pharmaceutical industry as medicine to treat different type of physiological complications [3-6]. The body prepares the important antioxidant from NAC by converting it firstly into L-Cys and then into glutathione [7]. Antioxidants such as or ascorbic acid (vitamin C) fight against the free radicals in our body and reduce oxidative stress before damage of the vital molecules. For healthy adults about 4.1 mg/kg/day of L-Cys is required as recommend by Joint FAO/WHO/UNO expert consultation [8]. Although L-Cys has a number of health benefits, the elevated amounts of such amino acid may cause neurotoxicity [9], promotes urinary stone formation [10] *etc.* and it can also be regarded as the biological marker for various diseases [11-13]. Therefore, it is of utmost importance to detect the concentration of L-Cys by a highly sensitive, selective and convenient method with high degree of accuracy in order to prevent its adverse effects in our health.

Various analytical methods such as immunoassay, electrochemistry, chromatography *etc.* are recently being explored for the detection of L-Cys and are performed in conjugation with liquid chromatography, fluorimetry, colorimetry, differential pulse voltammetry and spectrofluorimetry *etc.* [14-19]. But immunoassay and chromatography required expensive biological reagents and complicated instrumentations. Also the electrochemical methods show relatively low selectivity to L-Cys. Some methods utilize the fluorometric detection after direct labeling of suitable fluorescent probe with target bio-analyst. However direct labeling sometimes causes structural alternation of the biological species resulting erroneous

information. Also these detection methods directly utilizing the absolute fluorescence intensity sometimes may include unwanted noise due to environmental perturbation in the measurement. In recent times the colorimetric methods are attracted great attention but are still limited because of their lack of effectiveness at very low concentration. Therefore, it is of crucial importance to design the appropriate sensing platform for the detection of L-Cys both selectively and quantitatively with high degree of accuracy in the physiological range. In this direction, the method based on the fluorometric assay may offer great advantages for the detection of L-Cys as they enable a direct and level free detection in an aqueous environment even at very low concentration. Also the ratio-metric fluorescence recovery from the fully quenched state of any suitable fluorescent probe in presence of the analyst biomolecule ensures the elimination of any external perturbation involved in the measurements.

Metal nanoparticles are attracted considerable attention for their excellent ability to modulate the spectroscopic properties of various interesting cationic organic dyes in the aqueous environment [20, 21]. The ground and excited state electronic properties of such dye molecules adsorbed onto the surface of gold or silver nanoparticles show significant physical and physicochemical behavior which sometimes enable their use in many biomolecular recognition processes [22]. The reduction of excited state fluorescence life time down to several hundreds of picoseconds has been attributed to energy or electron transfer processes [23, 24] from excited dye molecules to these nanoparticles. The resonant coupling between the oscillatory electric dipole of plasmonic electrons and the dipole of excited dye molecules may be a possible reason for ultra-fast energy transfer [25]. These interesting photophysical processes of small organic dyes assembled on to the novel nanoparticle's surfaces are sometimes very sensitive to the specific guest-host geometry in a particular environment, which allows their possible application in the field of biosensors [26]. On the other hand, these nanoparticles may aggregate in solution while interacting with many biological

molecules namely protein, enzyme, amino acids *etc.* [27] resulting substantial effect on the surface plasmonic band under optical irradiation.

In this present report we address a highly sensitive and selective method for detection of L-Cys via fluorescence turn-off and turn-on mechanism based on the interaction of RhB and Au NPs in aqueous media. The cationic dye RhB belongs to xanthene family of organic dyes and has high fluorescence quantum yield (0.71) in water with good photo-stability [28, 29]. The fluorescence emission of RhB was turned on from its initial quenched state and was recovered (approximately 68 fold) after addition of L-Cys to RhB/Au NPs mixed solution at a concentration range between 0.01 µM to 1000 µM. Most interestingly this fluorometric method was accompanied with a significant and noticeable color changes of the final solution and is therefore a direct visual evidence for selective determination of L-Cys over all other associated amino acids in the aqueous medium.

2. Experimental

2.1. Materials

The amino acid of our interest i.e. L-Cys ($C_3H_7NO_2$, M.W: 121.15 $gmol^{-1}$) along with all other essential and non-essential amino acids used in this present work, RhB ($C_{28}H_{31}ClN_2O_3$, M.W: 479.02 $gmol^{-1}$), chlorauric acid ($HAuCl_4$, $3H_2O$, M.W: 339.79 $gmol^{-1}$), glutathione (M.W: 307.32 $gmol^{-1}$), ascorbic acid ($C_6H_8O_6$, M.W: 176.12 $gmol^{-1}$), uric acid ($C_5H_4N_4O_3$, M.W:168.11 $gmol^{-1}$) were purchased from Sigma Aldrich chemical company, USA and used without further purification. The purity of RhB was checked via spectroscopic method prior to use in the experiment. Trisodium citrate ($Na_3C_6H_5O_7$, M.W: 258.06 $gmol^{-1}$), sodium chloride (NaCl, M.W: 58.44 $gmol^{-1}$), potassium chloride (KCl, M.W: 74.5513 $gmol^{-1}$) were purchased from Merck Chemical Company, Germany. All the glasswares were cleaned with freshly prepared aquaregia solution (3:1 mixture of hydrochloric acid (HCl) and nitric

acid HNO_3) followed by subsequent rinsing with triple distilled deionized Milli-Q water (resistivity 18.2 MΩ cm, pH~7, collected from Synergy integrated with an Elix®-Advantage set-up, Millipore SAS, France) and then were autoclaved for 24 hours before use. Aqueous solutions of the chemicals were also prepared with the same triple distilled Milli-Q water.

2.2. Synthesis of Au NPs

Au NPs were synthesized by citrate reduction method as described elsewhere [30]. In a typical procedure, 50 ml aqueous solution of $HAuCl_4$, $3H_2O$ (concentration of 0.25 M) was heated to boiling and 1.2 ml of $Na_3C_6H_5O_7$ (1%) was added into the solution under vigorous stirring for preparing gold nanocolloidal solution. Within a time of 70 s, the boiling solution turned faintly to blue color and after 120 s the blue color changed to deep red. The solution was then set aside to cool down at room temperature. The final concentration of the gold nanocolloidal solution became 0.1 mM at pH ~7.

2.3. Characterizations techniques

The UV-Vis absorption spectra of the samples were recorded in the wavelength range of 200 - 800 nm by a double beam UV-Vis absorption spectrophotometer (UV-1800, Shimadzu, Japan) after proper baseline correction for the solvent background. Steady state fluorescence spectra of the samples were recorded in the range of wavelength 545-700 nm by using a Horiba Spectrofluorometer (Fluoromax-4C, Horiba Scientific Incorporated, USA). An excitation light source of wavelength 530 nm emerged through a slit having width of 2 nm was used for all the steady state fluorescence emission measurements. Both the absorption and emission spectra were collected from the sample solution in quartz cell (Kozima, Japan) of 1.0 cm path length at room temperature (25°C). The hydrodynamic nanoparticle size distribution and the effective surface Zeta potential (ζ) of the as-synthesized

Au NPs were obtained by a Zetasizer (Zetasizer Nano ZS, Malvern Instruments Ltd, UK) via dynamic light scattering method (DLS) at an ambient condition. High resolution TEM study of the Au NPs was carried out on a Transmission Electron Microscope (TEM) operated at 200 kV (JEM-2010 TEM, JEOL Ltd., Japan). For TEM study, the sample solutions were incubated for 15 minutes and then a small drop was spread onto the carbon coated copper microgrid (PELCO® 300 Mesh Grids, Ted Pella Inc. USA) and subsequently dried at room temperature. Time resolved fluorescence emission measurements were acquired by using time-correlated single photon counting (TCSPC) method (Fluorolog, Horiba Jobin Yvon, USA) to obtain the excited state fluorescence lifetime of the samples. In this method, the sample solutions were excited at 510 nm by using a picoseconds pulsed diode laser. The fluorescence decay data were collected over 200 channels which were calibrated on a non-linear time scale with increasing time according to an arithmetic progression with a Hamamatsu photomultiplier tube (R928P). The raw decay data as obtained were analyzed using IBH DAS6 software.

2.4. Method of fluorometric assay experiments

A 2 mL of 0.1 mM Au NPs solution was incubated at room temperature (25°C) for five minutes with the 2 mL of 0.1 μM RhB (probe molecules) solution so that the assay could be formed. Freshly prepared L-Cys solution of different concentration (1 mM - 0.01 μM) was added (200 μL) separately with the assay and kept for three minutes and subsequently the fluorescence spectra were recorded. For the colorimetric study, freshly prepared different amino acids, glutathione, uric acid, ascorbic acid and different neurotransmitters (K^+ and Na^+) stock solutions of concentration 0.1 mM were added with the assay and the color change was observed instantly. For confirmation of selectivity of the assay, mixture of freshly prepared mixed individual solutions of L-Cys and different amino acids, glutathione, uric

acid, ascorbic acid and neurotransmitters (in 1:1 volume ratio, concentration of 0.1 mM each) were added to the RhB/Au NPs solution and fluorescence emission was measured after three minutes for each mixed solutions.

3. Results and discussion

3.1. Characterization of synthesized Au NPs

Fig.1A shows the UV-Vis absorption spectrum of the citrate-stabilized Au NPs in aqueous colloidal solution and shows distinct absorption band with its maximum at around 528 nm along with two weak humps at 251 nm and 356 nm. The former is due to the strong characteristic surface plasmon resonance (SPR) while the other two are due to the intra-band electronic transitions of gold and can be related with the traces of such bands as similarly reported for silver nanoparticles by some researchers [31,32]. The well resolved and sharp SPR maximum band is basically due to both longitudinal and transverse SPR equivalently, which reveals a sign of the formation of spherical Au NPs. The molar extinction coefficient of Au NPs (with maximum SPR observed at 528 nm) was calculated as 540×10^{7} $M^{-1}cm^{-1}$ [33].

The DLS study (Fig.S1) revels that the average hydrodynamic size of Au NPs was about 53.78 nm. To have further knowledge about the homogeneity of NPs distributions the surface zeta potential (ζ) was measured (Fig.S2) and was found to be -30.1 mV at room temperature and solution pH ~7. These results suggest that Au NPs could overcome the van der Waal's attraction through the strong electrostatic repulsion between the negatively-charged citrate coronas around the NPs surface in aqueous medium and therefore Au NPs remained effectively stabilized prior to their use in the experiment [34].

However, to have a more precise and clear understanding of the size and morphology of Au NPs, TEM study was performed. Fig.1B shows that Au NPs were mono-dispersed with

nearly spherical in shape and the average particle diameter was ~27.5 nm as calculated from the size distribution curve (Fig.1C). The selected area electron diffraction (SAED) (Fig.1D) reveals the good crystalline nature of Au NPs. The rings as seen in SAED pattern were indexed and corresponds to the electron diffractions originated from (311), (222), (400) *etc.* planes of FCC gold crystal. The interplaner spacing as calculated (Fig.1D) was about 0.11 nm corresponding to the lattice plane (222). The High resolution-TEM micrograph was also shown in the inset of Fig.1D. The energy dispersive X-ray spectrum (EDS) curve (Fig.S3) shows the nucleation of Au NPs without any impurities and the presence of large number of Au NPs in its colloidal solution used for the experiment.

3.2. UV-Vis absorption spectroscopic study

The cationic dye RhB is a well-known laser dye from the xanthene family of organic dyes and its molecular structure is shown as the inset of Fig.2A. The UV-Vis absorption spectrum of pure RhB solution (concentration of 6 μM) as shown in Fig.2A (curve 3) exhibits a strong absorption band at around 554 nm which is attributed to the characteristic π-π* transition of dye monomer units and a very weak band observed at around 520 nm is assigned to the dimeric states of RhB molecules due to the n-π* transition [29]. In aqueous solution at low concentration (i.e. 6 μM) RhB dimmers are in equilibrium with the monomers and their mean numbers should remain constant at a particular concentration [29]. However, in our work, the concentration of RhB solution was about 0.1 μM for the detection of L-Cys. So it was presumed that most of the RhB molecules might exist as monomer units in the studied aqueous solution because of their very low concentration. RhB/Au NPs mixed solution (1:1 volume ratio) (Fig.2A, curve 2) showed that the main characteristic absorption band position (554 nm) of RhB was almost unaltered but with decreased intensity along with an increase in absorbance of dimeric band (520 nm) compared to that of pure RhB. This change in the

absorption spectrum of RhB in presence of Au NPs was possibly due to their adsorption on to the nanoparticles surface. More precisely this aggregation effects were manifested as the close packing of RhB dye molecules around the Au NPs surface and this eventually induced enhanced dye-dye intermolecular interaction. Some authors [20-22] also reported this type of aggregations of other xanthene family dyes on the Au NPs surface via strong electrostatic interaction. In fact, addition of Au NPs to the aqueous solution of RhB certainly changed the microenvironment around the electronic states of the dye molecules and this might have altered their electric transition dipole-moment. The interaction of molecular dipoles of RhB with the plasmonic field produced by Au NPs eventually affected the excitation energies of the individual dye molecules resulting decrease in absorbance of dye monomeric band at 554 nm.

The closer association of dye molecules on the Au NPs surface additionally induced the aggregations of NPs in the mixed sample which was also observed from TEM analysis (Fig.2B). It is clearly observed that different size of dye/Au composite systems were formed in the mixed ensembles which have been correlated with the observed UV-Vis results. The DLS measurement shows that the hydrodynamic diameter of the NPs increases after addition of RhB and the negative charges on the surface of citrate stabilized Au NPs were reduced as evidenced from Fig.S4 and Fig.S5 respectively.

3.3. Sensing of L-Cys based on fluorometric assay

In this work we systematically design a highly sensitive sensing platform for the quantitative as well as selective recognition of L-Cys using fluorometric assay of RhB/Au NPs in the aqueous medium. The sensing of L-Cys via fluorometric assay mechanism is schematically shown in Fig.3. The fluorescence emission spectra of RhB/Au NPs mixed aqueous solution (1:1 volume ratio) in absence (curve a) and presence (curve b) of L-Cys

(concentration of 100 μM) was shown in Fig.4A. It is observed that RhB/Au NPs mixed aqueous solution had negligibly small value of emission intensity because of efficient fluorescence resonance energy transfer (FRET) from excited dye molecules to the Au surface as well as also the decrease in radiative rate constant of individual RhB molecules adsorbed on NPs surface. The energy transfer from donor RhB to acceptor Au NPs is mainly due to FRET process which is clearly perceived from the large overlap between the emission of RhB and absorbance of Au NPs as shown in Fig.4B. However, most interestingly after addition of L-Cys solution to the RhB/Au NPs mixed solution the fluorescence emission at around 574 nm was found to emerge with much increased intensity from its quenched state as shown in Fig.4A (curve b). This observation clearly suggests that the emission of RhB molecules which were adsorbed onto the Au NPs surface before addition of L-Cys was recovered to a great extent and was possibly due to a strong interaction between L-Cys and Au NPs through the thiol moiety (-SH) [35]. Due to this strong affinity of thiol to Au NPs, the L-Cys molecules were strongly bound to NPs resulting the escape of RhB molecules away from NPs surface. Because the attachment of RhB molecules with Au NPs were due to electrostatic interaction whereas L-Cys tend to attach with Au NPs by Au-S bond via chemisorptions which is relatively much stronger. As a result, the electrostatic charge distribution around the NPs surface was disrupted causing the release of RhB molecules from Au NPs surface resulting the decrease of fluorescence quenching via nonradiative energy transfer. Thus addition of L-Cys eventually restored the fluorescence band intensity of RhB at around 574 nm. However, the control experiment (Fig.S6) (i.e. fluorescence emission of RhB/L-Cys mixed aqueous solution without Au NPs) reveals a negligible effect of L-Cys on the emission profile of RhB molecules in the studied aqueous medium as the unaltered emission band position and no such significant rise and fall of emission intensity with increase or decrease of L-Cys concentration. But the slight decrease in emission intensity of RhB after addition of

L-Cys solution of different concentrations might only be due to the dilution of the RhB concentration in the mixed solution and not due to any interaction in their ground or excited electronic states.

The aggregation of Au NPs was further evidenced from UV-Vis absorption spectroscopy as shown in Fig.4C. It was observed that an additional SPR band appeared at around 670 nm after addition of L-Cys [35] and intensity of the main SPR band at around 528 nm was sufficiently reduced compared to that in case of RhB/Au NPs mixed aqueous solution (Fig.2A, Curve 2). So the emergence of the new SPR band of RhB/Au NPs mixture in presence of L-Cys corresponded possible aggregation of Au NPs and have already been reported by A. Mocanu et. al. [36].

In order to support the above results as obtained from fluorometric assay method, TEM study (Fig.4D) was also performed for the RhB/Au NPs/L-Cys mixed solution at the same ambient condition. We already observed that the dye molecules were adsorbed on the Au NPs surface resulting some aggregation of Au NPs and the distribution became inhomogeneous (Fig.2B). However, from Fig.4D it is clearly observed that after addition of L-Cys in RhB/Au NPs mixed aqueous solution, the distribution of NPs became more homogeneous but the average size of the particle increased to about 40 nm. This increased size distribution of Au NPs was basically due to some aggregation of individual NPs in the relatively higher viscous medium after addition of L-Cys. However, the crystallinity of Au NPs after addition of L-Cys possibly was not altered as distinct diffraction rings was observed from SAED images (Inset of Fig.4D). DLS study as shown in Fig.S7 further reveals the increase in the hydrodynamic particle size distribution (~67.84 nm) of Au NPs in presence of RhB and L-Cys compared to pure Au NPs (~53.78 nm). Also the Zeta potential (ZP) (ζ) as measured for RhB/Au NPs/L-Cys mixed solution was found to be -13.0 mV (Fig.S8) which is much lower than that of pure Au NPs (-30.1 mV) as well as RhB/Au NPs

mixture (-20 mV). The reduced ZP of Au NPs in RhB/Au NPs/L-Cys mixture eventually favored further aggregation of NPs. More precisely the addition of L-Cys to the RhB/Au NPs mixed aqueous solution might have displaced the negatively charged citrate around NPs surfaces resulting the decrease in negative ZP of Au NPs. This in turn also favored the aggregation of Au NPs in aqueous medium [35].

Sensitivity of the proposed method

In the present work, we have also studied the quantitative detection of L-Cys via fluorometric assay of RhB/Au NPs assembly in the same aqueous environment. Fig.5 demonstrates the fluorescence spectra of RhB/Au NPs mixed aqueous solution in presence of various L-Cys concentrations viz. 0.01 µM, 0.1 µM, 1.0 µM, 10 µM, 100 µM and 1000 µM. From Fig.5, we immediately see that the fluorescence emission band of RhB at 574 nm was recovered and their intensity increased systemically with increase in L-Cys concentration. Also the increase in fluorescence recovery efficiency with the concentration of L-Cys was almost linear (Inset of Fig.5). The systematic recovery of fluorescence from RhB/Au NPs mixed solution in presence of L-Cys was highly sensitive with the change in the concentration of L-Cys. Therefore, this fluorometric assay in aqueous medium may be a suitable and efficient sensing platform for quantitative detection of amino acid L-Cys. The increased number of L-Cys molecules with increase in their concentration in RhB/Au NPs mixed solution definitely segregates more number of dye molecules from the surface of Au NPs and this has been manifested as the systematic linear increase in the fluorescence emission intensity. In fact, the initial quenched fluorescence emission of RhB due to Au NPs via FRET process was gradually decreased as the concentration of L-Cys was increased. A very good linear relationship between the fluorescence recovery efficiency (at 574 nm) and the concentration of L-Cys can be used to calibrate the proposed method of L-Cys detection

in the concentration range of 0.01 µM-0.1 mM as obtained from the inset of Fig.5. The calibration equation (eqn.1) for this approach can be written as

$$\mathrm{Log}[(F - F_0)/F_0] = \mathrm{Log}\,[C] + \text{ constant} \qquad \ldots\ldots\ldots\ldots (1)$$

where C is the concentration of L-Cys which was added into RhB/Au NPs mixed solution during the fluorometric assay experiments.

The linear fitted plot as shown in inset of Fig. 5 is almost passed through the initial point of the calibration curve and hence the limit of detection (LOD) may be approximately considered as 0.01 µM. The sensibility or the LOD of the proposed L-Cys detection method can be comparable with the results reported in the literature as cited in Table 1. Furthermore, the present technique utilizes the ratiometric fluorescence response of the fluorescent probe (RhB). Hence the effect of any impurity or external perturbation on the fluorescence was automatically discarded during the calibration of the proposed assay. Also the range of detection in the present method is comparable to the concentration of L-Cys present in the blood plasma [37] (near about micromolar), which suggests that our detection technique will have great potential with the diagnostic impact for biomedical interest.

Selectivity of the proposed method

In the practical purposes a good biosensor should selectively responds to a particular biological analyte which is to be sensed at a given time otherwise the sensing process will be failed to give the desired output. To evaluate the selectivity of the proposed method towards L-Cys, the interference of various other twenty amino acids such as L-Aspartate (L-Asp), L-Histidine (L-His), L-Methionine (L-Met), L-Serine (L-Ser), L-Tryptofan (L-Try), L-Alanine (L-Ala), L-Arginine (L-Arg), L-Glycine (L-Gly), L-Isolevcine (L-Iso), L-Proline (L-Pro), L-Threonine (L-Thr), L-Valine (L-Val), L-Asparagine (L-Aspa), L-Glutamic Acid (L-Glu), L-Glutamine (L-Glut), L-Phenylalanine (L-Phe), L-Leucine (L-Leu), L-Tyrosine (L-Tyr) and L-

Lysine (L-Lys), L-Homocysteine (L-HomoCys) and antioxidant glutathione (GSH) were tested via the same fluorometric assay method in aqueous medium. Apart from these amino acids, the interactions of other relevant biosamples such as uric acid and ascorbic acid and some neurotransmitters (K^+ and Na^+) are also examined with the proposed assay method.

Colorimetric response of the assay

The most interesting observation was that just after addition of equal amounts of various amino acids including L-Cys separately to the RhB/Au NPs mixed aqueous solution the color of the final solution became nearly bluish-black (as shown in Fig.6) only in case of L-Cys and could be clearly visualized with the naked eye. The concentrations of aqueous solutions of all the amino acids, other biosamples and neurotransmitters were same (0.1 mM) for these colorimetric observations. This was the initial visual evidence that L-Cys could selectively bind to Au NPs thereby changing the color of the final solution. It is already evident from Fig.4C (Curve b) that the addition of L-Cys to RhB/Au NPs mixed aqueous solution causes the emergence of the new absorption band of Au NPs at around 670 nm which implies a very fast and strong interaction between L-Cys and Au NPs in presence of probe RhB in the ground electronic states resulting the change of color of RhB/Au NPs mixed solution from wine to bluish-black.

Fig.7 shows the change in fluorescence recovery efficiency as a function of various amino acids including L-Cys as well as glutathione, uric acid, ascorbic acid and some neurotransmitters like Na^+, K^+ *etc.* and the corresponding emission spectra are shown in Fig.S9. From this plot it is clearly observed that the fluorescence recovery efficiency of RhB/Au NPs system in presence of L-Cys was significantly maximum compared to the rest of the amino acids although the concentration of all the amino acids remained same. The all other amino acids showed almost negligible effect on the quenched state of RhB adsorbed

onto Au NPs surface resulting no noticeable change in fluorescence intensity of the dye molecules. Additionally, there was no significant enhancement of fluorescence recovery efficiency while using the other amino acids of concentration of at least 100 times higher than that of pure L-Cys (Figure not shown). However, only other three essential amino acids namely L-Histidine, L-Methionine and L-Homocysteine showed slightly greater fluorescence recovery efficiency but still very less compared to the L-Cys. The slight difference of the fluorescence recovery efficiency in presence of L-Histidine and L-Methionine as shown in Fig.7 might be due to the electrostatic interaction of $-NH_2^+$with the negatively charged Au NPs and very minimal interaction through the less accessible intrabond S-atom resulting a slight decrease in overall fluorescence quenching via FRET between excited RhB molecules and Au NPs during photo excitation [38]. It is also relevant to mention here that it was unlikely for Au NPs to self-assemble with these two amino acids via covalent combination through S-Au bonds in the same aqueous environment as compared to L-Cys [39]. However, for L-Cys, the thiol moiety (-SH) is the head group and more exposed to aqueous environment causing greater extent of interaction with Au NPs. Although L-Homocysteine is a homologue of the amino acid L-Cys but differing with additional methylene bridge, it still shows almost 1/3 less fluorescence recovery efficiency compared to L-Cys while considering same molar concentrations for both the amino acids during the assay experiments. Additionally, the concentration of L-Homocysteine used was 0.1 mM which is much higher compared to its presence in real blood plasma. So it is excepted that in real biosample it would leave negligible effect in the detection of L-Cys by the proposed method.

In this work it is therefore highly important to study the relative fluorescence recovery efficiency of RhB/ Au NPs system when exposed to L-Cys in presence of other interfering essential and non-essential amino acids. This is because of the fact that the physiological plasma medium contains other amino acids as well along with L-Cys. So, the fluorescence

recovery efficiency study of RhB/Au NPs mixed aqueous solution was carried out in presence of L-Cys mixed with other amino acids (0.1 mM) and is shown in Fig.8. The corresponding emission spectra are also shown in Fig.S10 (supplementary information). Interestingly it has been observed that the fluorescence recovery efficiency from RhB/Au NPs mixed solution in presence of L-Cys mixed with various other amino acids was nearly equal or close to that obtained with pure L-Cys only. These results suggest that in the presence of L-Cys, approximately 20-fold enhancement of the fluorescence recovery efficiency was obtained when compared to that in presence of other amino acids without L-Cys in the mixture. From this study it can also be concluded that the presence of more freely assessable -S atoms in L-Cys compared to that in case of all other amino acids, L-Cys binds to Au NPs surface via S-Au bonding competitively and selectively in faster way resulting the displacement of RhB molecules from Au NPs surface. Consequently, the fluorescence quenching due to FRET between RhB and Au NPs was reduced. This is why fluorescence intensity became much higher when L-Cys was present with other amino acids in aqueous medium. Therefore, the proposed technique may be an efficient sensing platform for highly selective determination of amino acid L-Cys in aqueous medium.

Real bio-sample analysis by using the fluorometric assay

The proposed fluorescence based sensing mechanism for detection of L-Cys is also tested with real biosample in the present work. The L-Cys may present in both human blood plasma and urine. In our experiments we have used normal urine sample which was provided by our laboratory volunteer research student (male) having no renal complications. These experiments were performed with extra precaution to avoid any type of contamination or direct human contact with the urine sample. It is already known that [40] the excess amount of free L-Cys in urine causes the disease Cystinuria which leads to the formation of L-Cys

stones in the renal system. The same assay condition was maintained while doing the real sample analysis. The fluorescence recovery efficiencies were measured from the RhB/Au NPs system in presence of pure human urine, L-Cys and other amino acid mixed urine and are shown in Fig. 9. The corresponding fluorescence emission spectra are shown in Fig.S11. From Fig.9 it is observed that, the assay experiment with just pure urine sample shows nearly 35% fluorescence recovery whereas addition of L-Cys (0.1 mM, 200 µL) to the urine shows enhancements of fluorescence recovery efficiency up to 62%. The normal level of L-Cys in human urine is about 0.13 mmol/day [41] and any excess amount of L-Cys in the urine is therefore manifested as several health issues. Therefore, the initial fluorescence recovery with pure urine sample is basically due to usual presence of L-Cys in the urine. However, the increase of fluorescence recovery efficiency after addition L-Cys in the urine is a confirmation of selective detection of L-Cys because presence of all other amino acid did not show any significant rise in fluorescence recovery efficiency as observed from Fig. 9. Thus the present mechanism may be a suitable method for the determination of L-Cys in the human urine sample in order to diagnose the disease Cystinuria.

3.4. Time resolved fluorescence emission spectroscopy study

The time resolved fluorescence emission spectroscopy is a useful and powerful method to know the excited state life time of fluorophore and the nature of quenching whether it is dynamic or static. In this study, the time resolved fluorescence emission of RhB aqueous solumintion (0.1 µM) was measured by using Time correlated single photon counting (TCSPC) method in absence and presence of Au NPs and L-Cys respectively using an excitation laser source of wavelength of 510 nm and the corresponding fluorescence emission was monitored at 574 nm. The fluorescence decay plots as obtained were fitted by

two exponential functions according to eqn.2 and are shown in Fig.10. The average lifetimes of the samples were calculated according to eqn. 3 [23] and are summarized in Table 2.

$$I(t) = \alpha_1 e^{-t/\tau_1} + \alpha_2 e^{-t/\tau_2} \quad \ldots\ldots\ldots\ldots \quad (2)$$

$$\tau_{av} = \frac{\sum_i \alpha_i \tau_i^2}{\sum_i \alpha_i \tau_i} \ldots\ldots\ldots\ldots \quad (3)$$

where α_1, α_2 are the normalized pre-exponential factor of the molecules with lifetime τ_1 and τ_2 respectively. τ_{av} is the average fluorescence life time. The average fluorescence life time of pure RhB was calculated as 1.384 ns [29] but it was decreased to 1.225 ns after the addition of Au NPs (0.1 mM). This decrease in fluorescence lifetime might be related to the reduced excited state energy of RhB molecules due to their adsorption onto Au NPs surface in solution as well as the non-radiative energy transfer from RhB to Au NPs and some extent of dye aggregation. The relationship between the intensity of fluorescence emission and the life time of fluorophore may be given as in eqn.4 [36]

$$\tau_{obs} = \frac{1}{K_{obs}} = \frac{1}{K_r + K_{nr} + K_{et}} \quad \ldots\ldots\ldots\ldots\ldots \quad (4)$$

That is the observed lifetime τ_{obs} is the inverse of the observed decay rates, radiative decay rate K_r, non-radiative decay rate K_{nr} and the rate of energy transfer K_{et}. For a particular organic dye in specific environment, both the radiative and non-radiative decay rates are normally considered as constant. From the steady state measurement, it was already observed that the decrease in radiative rate of RhB upon adsorption on to Au NPs was only 20% to the overall fluorescence quenching. Thus the rate of energy transfer K_{et} is the major contributor to the decreased fluorescence lifetime of the fluorophore in presence of the Au NPs which played the dominant role in fluorescence quenching. However, the most interesting observation was that when L-Cys solution was added to the RhB/Au NPs mixed solution the average fluorescence lifetime of RhB molecules was again enhanced significantly to 1.342 ns which is almost close to that of pure dye molecules. More precisely the reversal of the

fluorescence lifetime of RhB after addition of L-Cys is basically attributed to the availability of free RhB molecules in the surrounding aqueous medium of Au NPs/L-Cys conjugated systems. Therefore, this result also supports the fluorescence recovery of RhB molecules from their quenched state in the surface of Au NPs when exposed to L-Cys solution. The very small difference in the average lifetime in this case as compared to that of pure RhB may be due to the different microenvironment of the surrounding medium of dye molecules after addition of L-Cys because the dielectric properties of the medium might have changed [42]. This may slightly affect the decay path of the excited RhB molecules.

4. Conclusion

We have successfully developed a sensing platform for selective and quantitative detection of important bio-thiol namely L-Cys via fluorometric assay of RhB and Au NPs in aqueous medium as well as in real biosample (human urine). The LOD for L-Cys was found to be 0.01 μM in our experimental range of concentration. The initial fluorescence quenching of RhB in presence of Au NPs without L-Cys in the mixture was possibly dominated by FRET mechanism which depends upon the relative distance between dye and nanoparticles. As the decrease in the radiative rate of RhB/Au NPs complex systems contributed only 20 % of the overall fluorescence quenching, which also suggest that the excited state energy transfer was dominant factor for the drastic fluorescence quenching. The selective fluorescence response of RhB/Au NPs complex molecular assemblies in presence of L-Cys in the mixture was also accompanied with a color change from wine to bluish-black which was not observed for all other amino acids including other thiol containing compounds, namely L-Methionine, L-Homocysteine, glutathione in the same aqueous environment. Additionally, the other relevant biosamples such as uric acid, ascorbic acid, neurotransmitters have shown negligible interference over the selective determination of L-Cys. However, the assay with

real biosample shows about 35 % fluorescence recovery occurred from the mixture. This is basically due to usual presence of L-Cys in normal urine. In aqueous solution the thiol moiety in L-Cys formed strong bonding with the citrate caped Au NPs and might have displaced RhB molecules from the surface of Au resulting the aggregation of individual NPs as confirmed by UV-Vis absorption spectroscopy. The TEM study confirmed that our synthesized Au NPs was nearly spherical with average diameter of 27.5 nm. DLS and Zeta potential studies revealed the homogeneity of Au NPs distribution in aqueous solution and did not aggregate prior to their use in the experiments. Fluorescence lifetime of RhB adsorbed onto Au NPs surface was reduced compared to that of pure RhB in aqueous solution as confirmed by TCSPC study. Addition of L-Cys in the mixture restored the fluorescence lifetime of pure RhB resulting the decrease of fluorescence quenching via FRET. Therefore, the present study may be proposed as an efficient sensing platform for selective and highly sensitive detection of L-Cys via fluorometric assay mechanism using Au NPs and RhB.

Acknowledgements

Authors P. Maiti and P. K. Paul are grateful to West Bengal State Council of Science and Technology (WBSCST), Govt. of West Bengal for financial assistance (Project Ref. No. 493/WBSCST/F/0545/15(Pt-I) to perform this work. P. K. Paul also thankful to SERB DST, Govt. of India for finical assistance through project SB/EMEQ-142/2014. Authors are grateful to CSS of Indian Association for the Cultivation of Science, Kolkata for providing HR TEM facility used in this work. S. A Hussain is also thankful to SERB DST, Govt. of India for finical support through project Ref. No. EMR/2014/000234.

References

[1] E.G. Schulz, H.R. Schirmer, Principles of Protein Structure, first ed., Springer, New York, 1978.

[2] W. Wang, O. Rusin, X. Xu, K.K. Kim, O.J. Escobedo, O.S. Fakayode, A.K. Fletcher, M. Lowry, M.C. Schowalter, M.C. Lawrence, R.F. Fronczek, M.I. Warner, M.R. Strongin, Detection of homocysteine and cysteine, J. Am. Chem. Soc. 127 (2005) 15949-15958.

[3] K.J. Nicholson, J. Connelly, C.J. Lindon, E. Holmes, Metabonomics: a platform for studying drug toxicity and gene function, Nat. Rev. Drug Discov. 1 (2002) 153-161.

[4] K.R. Atkuri, J.J. Mantovani, L.A. Herzenberg, L.A. Herzenberg, N-Acetylcysteine-a safe antidote for cysteine/glutathione deficiency, Curr Opin. Pharmacol,7 (2007) 355-359.

[5] S.K. Biswas, I. Rahman, Environmental toxicity, redox signaling and lung inflammation: the role of glutathione, Mol. Aspects Med. 30 (1-2) (2009) 60-76.

[6] R.V. Kondratov, O. Vykhovanets, A.A. Kondratova, M.P. Antoch, Antioxidant N-acetyl-l-cysteine ameliorates symptoms of premature aging associated with the deficiency of the circadian protein BMAL1, Aging 1(12) (2009) 979-987.

[7] V.I. Lushchak, Glutathione homeostasis and functions: potential targets for medical interventions, J. Amino Acids. 2012 (2011) 1-26.

[8] World Health Organization, Food and Agriculture Organization of the United Nations, United Nations University, Protein and amino acid requirements in human nutrition, WHO, 2002, http://www.who.int/iris/handle/10665/43411.

[9] R. Janáky, V. Varga, A. Hermann, P. Saransaari, S.S. Oja, Mechanisms of L-cysteine neurotoxicity, Neurochem. Res. 25 (9-10) (2000) 1397-1405.

[10] J.D. Rimer, Z. An, Z. Zhu, M.H. Lee, D.S. Goldfarb, J.A. Wesson, M.D. Ward, Crystal growth inhibitors for the prevention of l-cystine kidney stones through molecular design, Science 330 (6002) (2010) 337-341.

[11] B. Halliwel, Reactive Oxygen species in living systems: source, biochemistry, and role in human disease, Am. J. Med. 91 (1991) 14-22.

[12] J.T. Jarrett, The biosynthesis of thiol- and thioether-containing cofactors and secondary metabolites catalyzed by radicals-adenosylmethionine enzymes, J. Biol. Chem. 290 (2015) 3972-3979.

[13] E. Mukwevho, Z. Ferreira, A. Ayeleso, Potential role of sulfur-containing antioxidant systems in highly oxidative environments, Molecules 19 (2014) 19376-19389.

[14] R. Glowacki, J. Stachniuk, K. Borowczyk, A simple HPLC-UV method for simultaneous determination of cysteine and cysteinylglycine in biological fluids, Acta Chromatogr, 28 (2016) 333-346.

[15] M. Bouri, R. Salghi, A. Rios, M. Zougagh, Fluorescence determination of L-cysteine in wound dressings by fluoroscein coated gold nanoparticles, Anal. Lett. 49 (2016) 1221-1232.

[16] Z. Huang, Y. Yang, Y, Long, H. Zheng, A colorimetric method for cysteine determination based on the peroxidase-like activity of ficin, Anal. Methods 10 (2018) 2676-2680.

[17] G. Ziyatdinova, E. Kozlova, H. Budnikov, Selective electrochemical sensor based on the electropolymerized pcoumaric acid for the direct determination of L-cysteine, Electrochimica Acta 270 (2018) 369-377.

[18] L. Chang, T. Wu, F. Chen, Determination of L-cysteine base on the reversion of fluorescence quenching of calcein by copper(II) ion, Microchim Acta 177 (2012) 295-300.

[19] A.A. Ensafi, B. Rezaei, S. Nouroozi, Flow injection spectrofluorometric determination of cystine and cysteine, J. Braz. Chem. Soc. 20 (2009) 288-293.

[20] N. Narband, M. Uppal, C.W. Dunnill, G. Hyett, M. Wilson, I.P. Parkin, The interaction between gold nanoparticles and cationic and anionic dyes: enhanced uv-visible absorption, Phys. Chem. Chem. Phys. 11 (2009) 10513-10518.

[21] N. Kometani, M. Tsubonishi, T. Fujita, K. Asami, Y. Yonezawa, Preparation and optical absorption spectra of dye-coated Au, Ag, and Au/Ag colloidal nanoparticles in aqueous solutions and in alternate assemblies, Langmuir 17 (2001) 578-580.

[22] M.C. Daniel, D. Astruc, Gold nanoparticles: assembly, supramolecular chemistry, quantum-size-related properties, and applications toward biology, catalysis, and nanotechnology, Chem. Rev. 104 (2004) 293-346.

[23] J.R. Lakowicz, Principles of Fluorescence Spectroscopy, third ed., Plenum Press, New York, 1983.

[24] D. Gust, T.A. Moore, A.L. Moore, Molecular mimicry of photosynthetic energy and electron transfer, Acc. Chem. Res. 26 (1993) 198-205.

[25] F. Tam, G.P. Goodrich, B.R. Johnson, N.J. Halas, Plasmonic enhancement of molecular fluorescence, Nano Lett. 7 (2007) 496-501.

[26] P.C. Ray, Size and shape dependent second order nonlinear optical properties of nanomaterials and their application in biological and chemical sensing, Chem. Rev. 110 (9) (2010) 5332-5365.

[27] R.A. Sperling, W.J. Parak, Surface modification, functionalization and bioconjugation of colloidal inorganic nanoparticles, Philos. Trans. Royal Soc. A 368 (2010) 1333-1383.

[28] T. Karstens, K. Kobs, Rhodamine B and rhodamine 101 as reference substances for fluorescence quantum yield measurements, J. Phys. Chem. 84 (14) (1980) 1871-1872.

[29] N.K.M.N. Srinivas, S.V. Rao, D.N. Rao, Saturable and reverse saturable absorption of rhodamine b in methanol and water, J. Opt. Soc. Am. B, 20 (12) (2003) 2470-2479.

[30] G. Frens, Controlled nucleation for the regulation of the particle size in monodisperse gold suspensions, Nat. Phys. 241 (1973) 20-22.

[31] X.C. Ma, Y. Dai, L. Yu, B.B. Huang, Energy transfer in plasmonic photocatalytic composites, Light Sci. Appl. 5 (2016) 16017-16029.

[32] S.D. Roy, M. Ghosh, J. Chowdhury, Adsorptive parameters and influence of hot geometries on the SER(R)S spectra of methylene blue molecules adsorbed on gold nanocolloidal particles, J. Raman Spectrosc. 46 (2015) 451-461.

[33] N.R. Jana, L. Gearheart, C.J. Murphy, Seeding growth for size control of 5-40 nm diameter gold nanoparticles, Langmuir 17 (2001) 6782-6786.

[34] W. Zhao, M.A. Brook, Y. Li, Design of gold nanoparticle-based colorimetric biosensing assays, ChemBioChem. 9 (2008) 2363-2371.

[35] F. Chai, C. Wang, T. Wang, Z. Ma, Z. Su, L-cysteine functionalized gold nanoparticles for the colorimetric detection of hg^{2+} induced by ultraviolet light, Nanotechnology 21 (2010) 25501-25506.

[36] A. Mocanu, I. Cernica, G. Tomoaia, L.D. Bobos, O. Horovitz, M.T. Cotisel, Self-assembly characteristics of gold nanoparticles in the presence of cysteine, Colloids Surf. A: Physicochem. Eng. Asp. 338 (2009) 93-101.

[37] J.W. Olney, C. Zorumski, M.T. Price, J. Labruyere, L-cysteine, a bicarbonate sensitive endogenous excitotoxin, Science 248 (1990) 596-599.

[38] R. Cao, B. Li, A simple and sensitive method for visual detection of heparin using positively-charged gold nanoparticles as colorimetric probes, Chem. Commun. 47 (2011) 2865-2867.

[39] M. Bahram, E. Mohammadzadeh, Green synthesis of gold nanoparticles with willow tree bark extract: a sensitive colourimetric sensor for cysteine detection, Anal. Methods 6 (2014) 6916-6924.

[40] E. Kaniowska, G. Chwatko, R. Głowacki, P. Kubalczyk, E. Bald, Urinary excretion measurement of cysteine and homocysteine in the form of their S-pyridinium derivatives by high-performance liquid chromatography with ultraviolet detection, J. Chromatogr. A 798 (1998) 27-35.

[41] C.S. Biyani, J.J. Cartledge, Cystinuria-Diagnosis and Management, EAU-EBU Update Series 4 (2006) 175-183.

[42] H. Chen, S.S. Ahsan, M.E.B.S. Berrios, H.D. Abrun, W.W. Webb, Mechanisms of quenching of alexa fluorophores by natural amino acids, J. Am. Chem. Soc. 132 (2010) 7244-7245.

Figure captions

Fig.1 (A) UV-Vis absorption spectrum of Au NPs in aqueous colloidal solution (concentration of 0.1 mM). (B) TEM micrograph of as-synthesized mono-dispersed Au NPs desiccated at room temperature, (C) Lognormal fitting of the particle size distribution, (D) SAED pattern with the Miller-indices of Au NPs. Inset of (D) shows the HR TEM micrograph with crystal spacing.

Fig.2 (A) UV-Vis absorption spectra of (1) aqueous colloidal dispersion of Au NPs (0.1 mM), (2) mixed aqueous solution of RhB (6 µM) and Au nanocolloidal solution (0.1 mM), (3) aqueous solution of pure RhB (6 µM). Inset shows the molecular structure of RhB dye. (B) TEM micrograph of RhB mixed Au NPs showing the aggregation of Au NPs. Inset shows the corresponding SAED pattern which suggests that the crystallinity of the Au NPs was not lost due to the adsorption RhB molecules onto their surface.

Fig.3 Mechanism of detection of L-Cys using fluorometric assay.

Fig.4 (A) Fluorescence emission spectrum from the assay of RhB/Au NPs in absence (curve a) and presence (curve b) of L-Cys, (B) Overlapping between normalized emission spectrum of RhB (curve 2) and absorption spectrum of Au NPs (curve 1), (C) UV-Vis absorption spectra of RhB/Au NPs mixed solution (0.1 mM & 0.1µM in 1:1 volume ratio) in absence (curve a) and presence (curve b) of L-Cys. Inset shows the UV-Vis absorption spectrum of RhB (0.1 µM) in presence of L-Cys (0.1 mM), (D) TEM micrograph of RhB/Au NPs/L-Cys mixed sample. Inset shows the corresponding SAED pattern,

Fig.5 Fluorescence recovery from assay of RhB/Au NPs in presence of L-Cys of various concentration viz. 0.01 µM (2), 0.1 µM (3), 1.0 µM(4), 10 µM (5), 100 µM (6) and 1000 µM (7). The spectrum (1) represents florescence emission of RhB/Au NPs mixed solution. Inset shows the plot of Log[fluorescence recovery efficiency] versus Log [L-Cys concentration].

Fig.6 Digital photographs of RhB/Au NPs mixed solution before (Control) and after adding of all twenty amino acids, glutathione, uric acid, ascorbic acid and neurotransmitters. Images reveal a direct visual evidence for the color change (from wine to bluish black) only for L-Cys solution in the mixed ensemble.

Fig.7 Relative fluorescence recovery efficiency of the assay of RhB/Au NPs at 574 nm upon addition of L-Cys and other amino acids, glutathione, uric acid, ascorbic acid and neurotransmitters.

Fig.8 The plot of relative fluorescence recovery efficiency (at 574 nm) from the assay of RhB/ Au NPs when exposed to the aqueous solution of L-Cys (0.1 mM) mixed with other amino acids (0.1 mM), glutathione (0.1 mM), uric acid (0.1 mM), ascorbic acid (0.1 mM) and neurotransmitter (0.1 mM). Figure also represents the relative fluorescence recovery efficiency of the assay when added separately with other amino acids (0.1 mM), glutathione (0.1 mM), uric acid (0.1 mM), ascorbic acid (0.1 mM) and neurotransmitters (0.1 mM)

Fig.9 Real biosample analysis by using the fluorometric assay with pure human urine and amino acids.

Fig.10 Fluorescence decay plots of pure RhB aqueous solution and of RhB/Au NPs mixed solution in absence and presence of L-Cys.

Figures

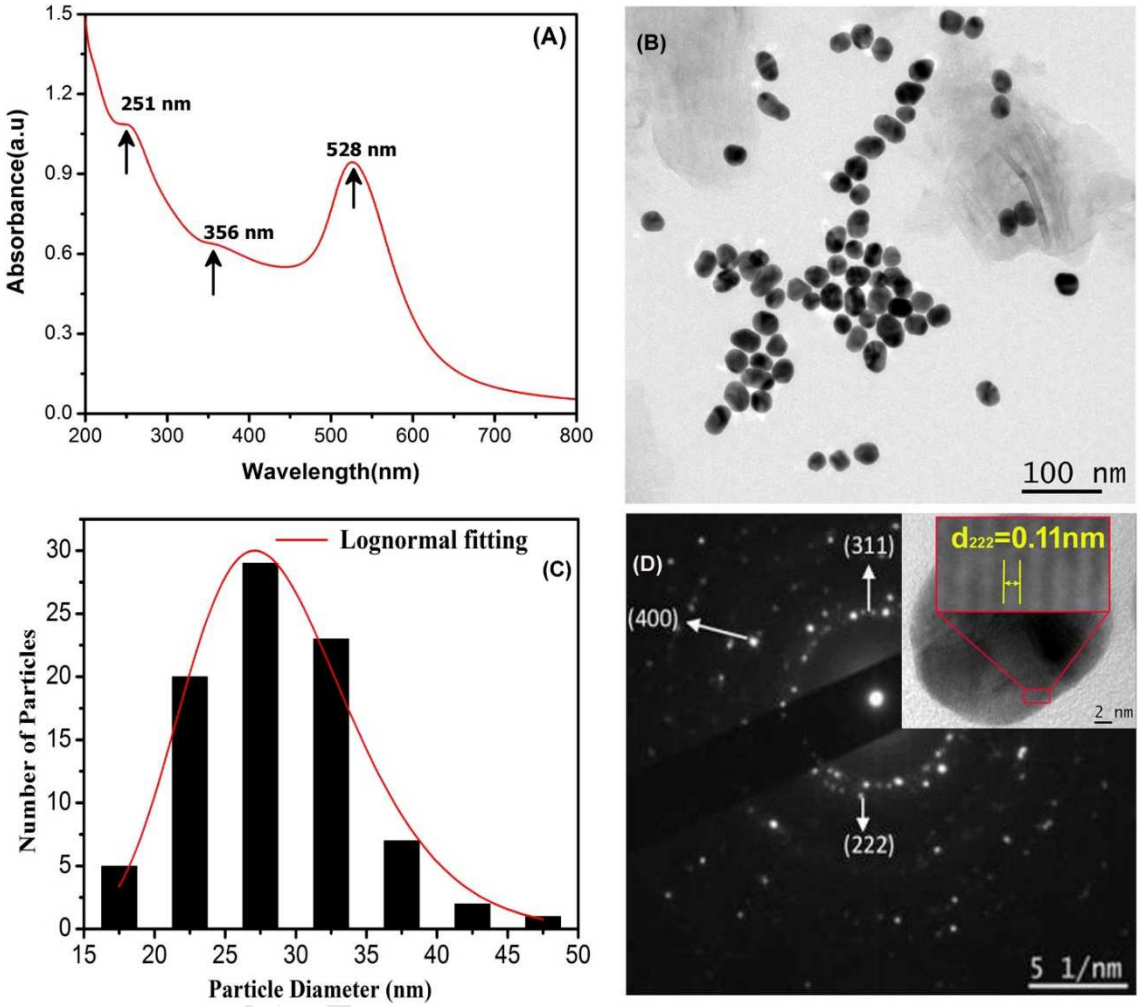

Fig.1(A) UV-Vis absorption spectrum of Au NPs in aqueous colloidal solution (concentration of 0.1 mM). (B) TEM micrograph of as-synthesized mono-dispersed Au NPs desiccated at room temperature, (C) Lognormal fitting of the particle size distribution, (D) SAED pattern with the Miller-indices of Au NPs. Inset of (D) shows the HR TEM micrograph with crystal spacing.

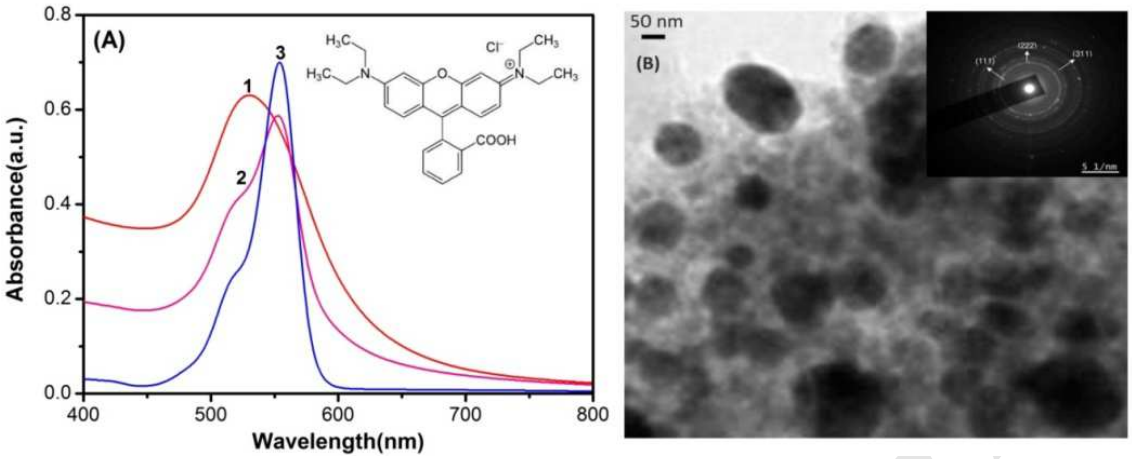

Fig.2 (A) UV-Vis absorption spectra of (1) aqueous colloidal dispersion of Au NPs (0.1 mM), (2) mixed aqueous solution of RhB (6 µM) and Au nanocolloidal solution (0.1 mM), (3) aqueous solution of pure RhB (6 µM). Inset shows the molecular structure of RhB dye. (B) TEM micrograph of RhB mixed Au NPs showing the aggregation of Au NPs. Inset shows the corresponding SAED pattern which suggests that the crystallinity of the Au NPs was not lost due to the adsorption RhB molecules onto their surface.

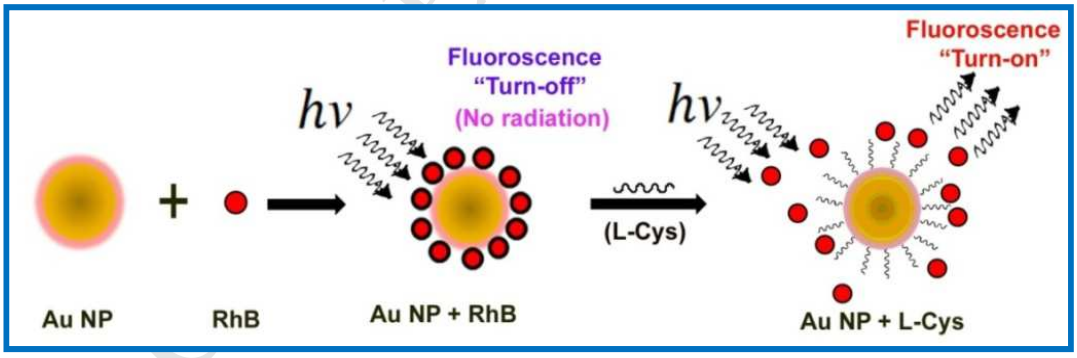

Fig.3 Mechanism of detection of L-Cys using fluorometric assay.

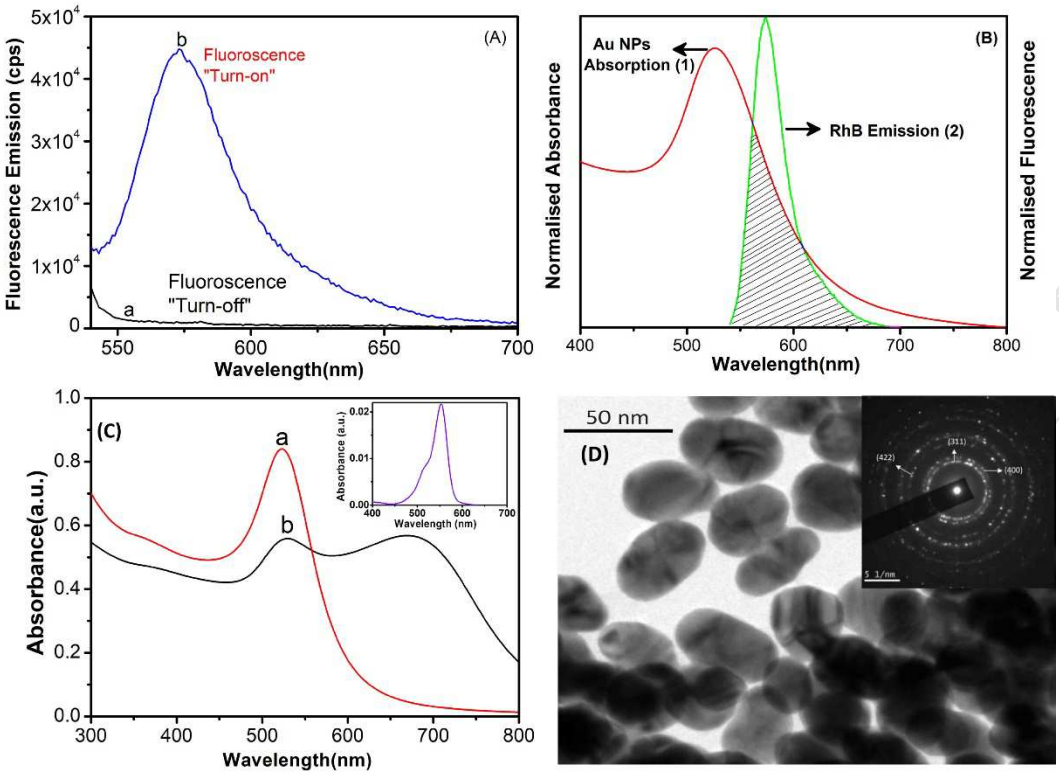

Fig.4 (A) Fluorescence emission spectrum from the assay of RhB/Au NPs in absence (curve a) and presence (curve b) of L-Cys, (B) Overlapping between normalized emission spectrum of RhB (curve 2) and absorption spectrum of Au NPs (curve 1), (C) UV-Vis absorption spectra of RhB/Au NPs mixed solution (0.1 mM & 0.1 µM in 1:1 volume ratio) in absence (curve a) and presence (curve b) of L-Cys. Inset shows the UV-Vis absorption spectrum of RhB (0.1 µM) in presence of L-Cys (0.1 mM). (D) TEM micrograph of RhB/Au NPs/L-Cys mixed sample. Inset shows the corresponding SAED pattern.

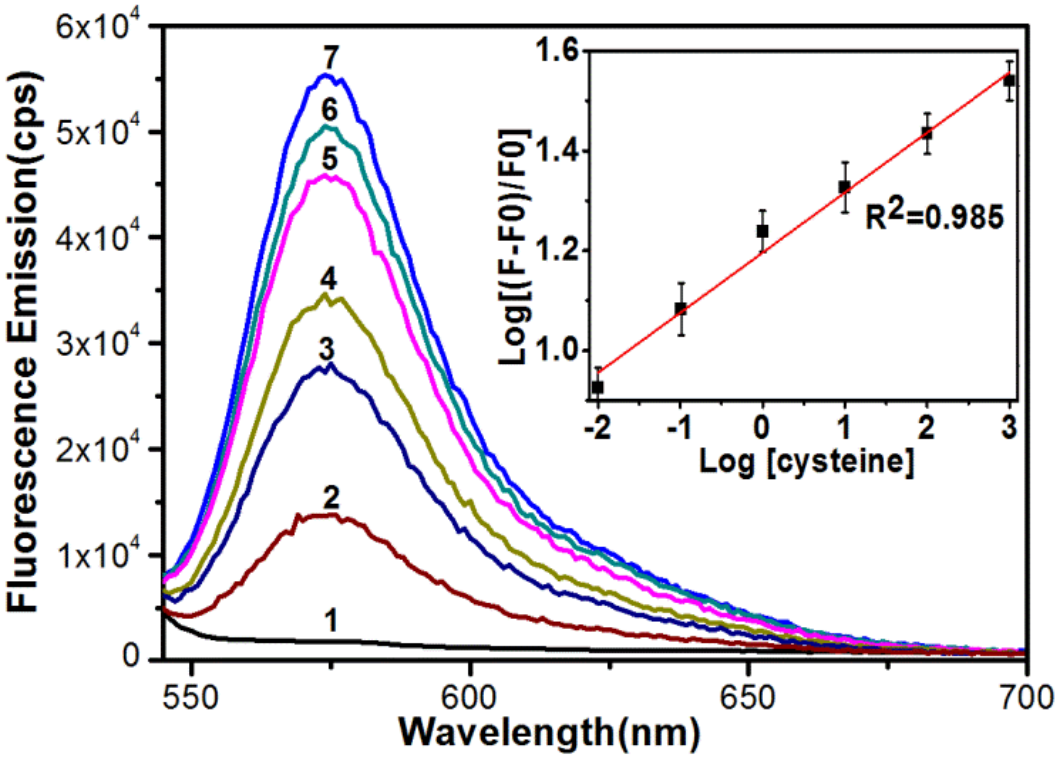

Fig.5 Fluorescence recovery from assay of RhB/Au NPs in presence of L-Cys of various concentration viz. 0.01 µM (2), 0.1 µM (3), 1.0 µM(4), 10 µM (5), 100 µM (6) and 1000 µM (7). The spectrum (1) represents florescence emission of RhB/Au NPs mixed solution. Inset shows the plot of Log[fluorescence recovery efficiency] versus Log [L-Cys concentration].

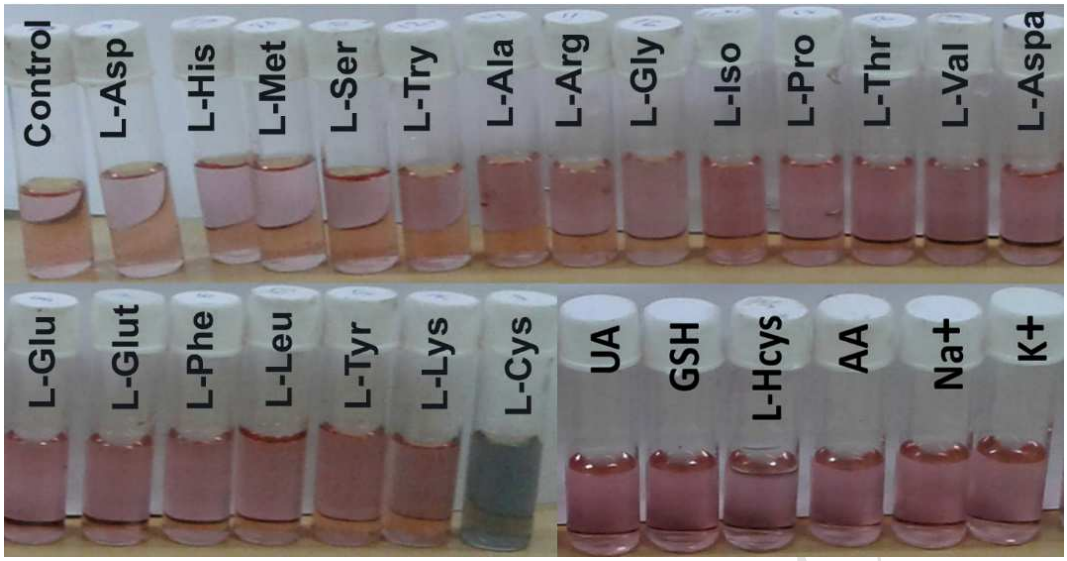

Fig.6 Digital photographs of RhB/Au NPs mixed solution before (Control) and after adding of all twenty amino acids, glutathione, uric acid, ascorbic acid and neurotransmitters. Images reveal a direct visual evidence for the color change (from wine to bluish black) only for L-Cys solution in the mixed ensemble.

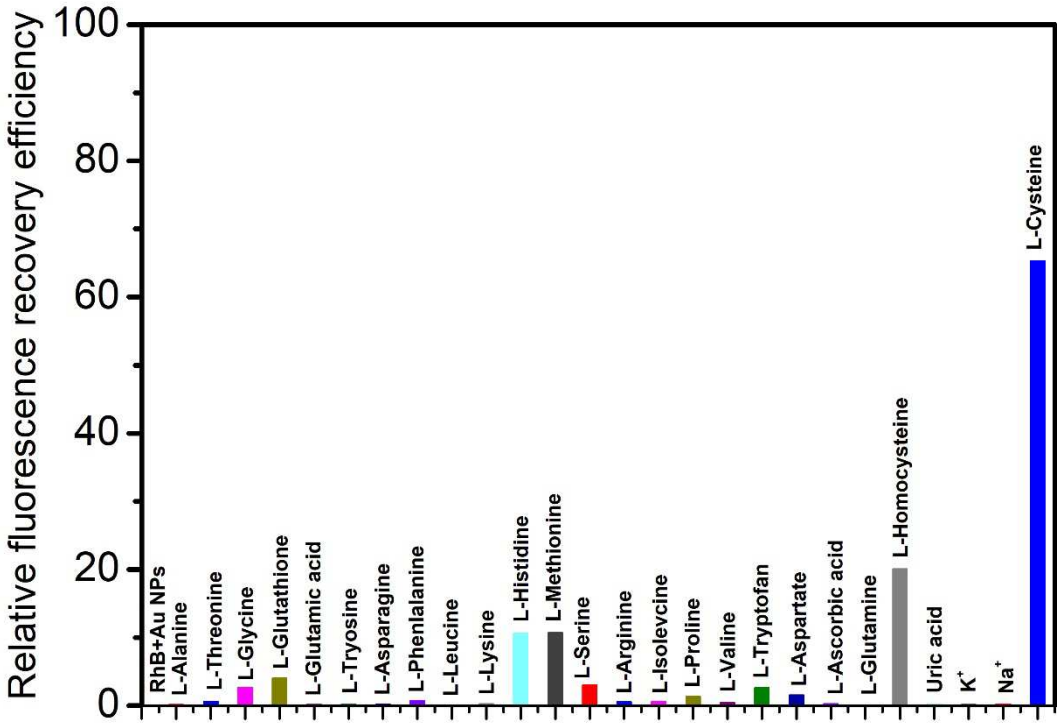

Fig.7 Relative fluorescence recovery efficiency of the assay of RhB/Au NPs at 574 nm upon addition of L-Cys and other amino acids, glutathione, uric acid, ascorbic acid and neurotransmitters.

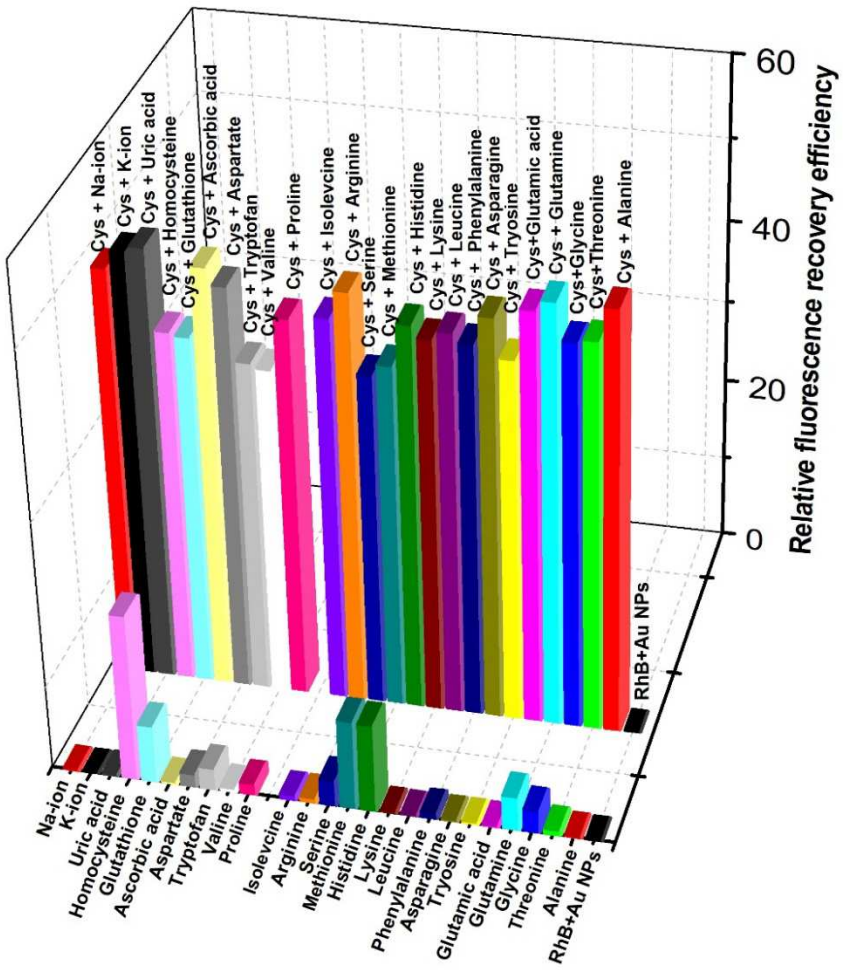

Fig.8 The plot of relative fluorescence recovery efficiency (at 574 nm) from the assay of RhB/ Au NPs when exposed to the aqueous solution of L-Cys (0.1 mM) mixed with other amino acids (0.1 mM), glutathione (0.1 mM), uric acid (0.1 mM), ascorbic acid (0.1 mM) and neurotransmitter (0.1 mM). Figure also represents the relative fluorescence recovery efficiency of the assay when added separately with other amino acids (0.1 mM), glutathione (0.1 mM), uric acid (0.1 mM), ascorbic acid (0.1 mM) and neurotransmitters (0.1 mM).

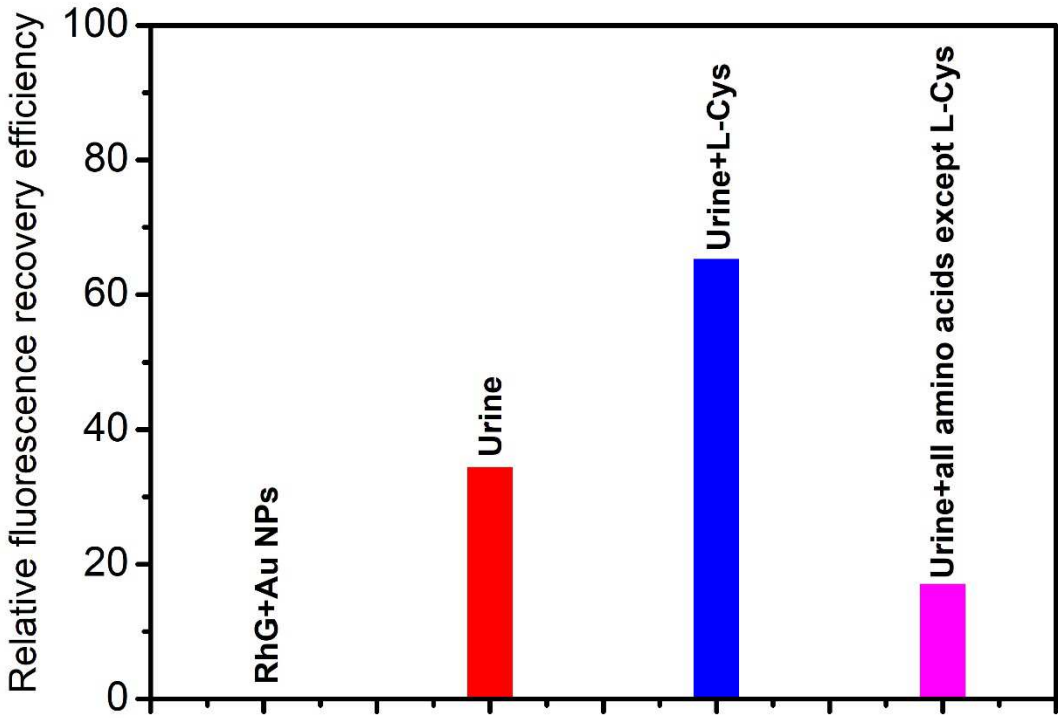

Fig.9 Real biosample analysis by using the fluorometric assay with pure human urine and amino acids.

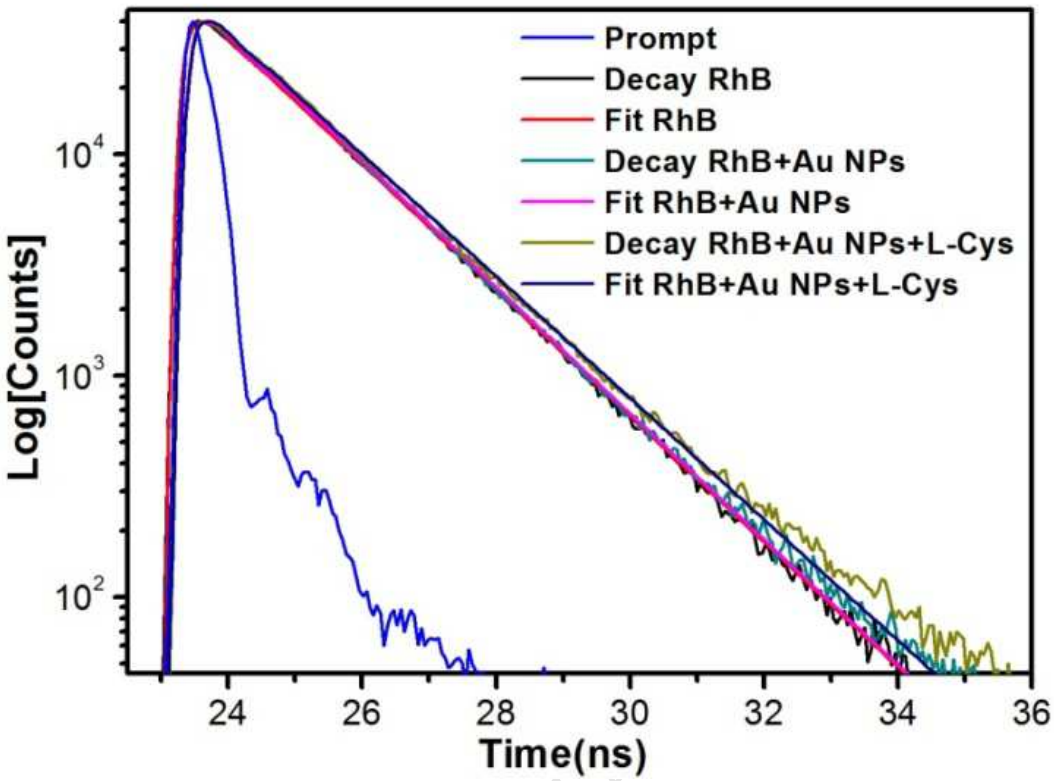

Fig.10 Fluorescence decay plots of pure RhB aqueous solution and RhB/Au NPs mixed solution in absence and presence of L-Cys.

Table 1

Comparison with other reported methods for detection of L-Cys.

Probe	Detection principle	Range (in μM)	LOD (μM)	References
TCEP & CMQT*	HPLC-UV	20 - 300	0.5	[14]
Fluorescein–modified gold nanoparticles	Fluorescence	0.8 - 4.1	0.1	[15]
Ficin	Colorimetry	0.05 - 14	0.02	[16]
Poly(p-coumaric acid)/MWNT/GCE**	Differential pulse voltammetry	7.5 - 1000	1.1	[17]
Cu^{2+}-caclein	Fluorimetry	0.3 - 12	0.04	[18]
Tl(III)***	Spectrofluorimetry	0.1 - 5.5	0.1	[19]
Rhodamine B Coated Au NPs	Fluorometric assay	0.01 – 100	0.01	**This work**

*TCEP - tris(2-carboxyethyl)phosphine hydrochloride, CMQT - 2-Chloro-1-thylquinolinium tetrafluoroborate, **MWNT/GCE - multi-walled carbon nanotubes modified glassy carbon electrode, ***Tl(III) - Thallium(III).

Table 2

Fluorescence life time parameters as obtained from the fitted data of pure RhB and RhB/Au NPs mixed solution in absence and presence of L-Cys. Corresponding fluorescence emission was monitored at 574 nm.

Sample name	**Number of Exponential**	λ_{ex} **(nm)**	τ_1 **(ns)**	α_1	τ_2 **(ns)**	α_2	τ_{av} **(ns)**	χ^2
RhB	2	510	0.066	0.375	1.522	0.156	1.384	1.276
RhB/Au NPs	2	510	0.037	1.311	1.517	0.129	1.225	1.156
RhB/Au NPs/L-Cys	2	510	0.048	0.788	1.577	0.132	1.342	1.279

λ_{ex}= Excitation wavelength

Highlights

- ✓ Gold nanoparticles can sufficiently quench the fluorescence of Rhodamine B dye
- ✓ L-Cysteine was detected selectively from fluorescence of dye/nanoparticle mixture
- ✓ Selective fluorescence response was accompanied with an observable colour change
- ✓ The calibration curve for the assay of L-Cysteine was almost linear
- ✓ Selective response of L-Cysteine in real human urine sample via fluorometric assay